

## HINTS OF DYNAMICAL VACUUM ENERGY IN THE EXPANDING UNIVERSE

JOAN SOLÀ<sup>1,2</sup>, ADRIÀ GÓMEZ-VALENT<sup>1,2</sup>, JAVIER DE CRUZ PÉREZ<sup>1</sup>

*Draft version September 4, 2015*

### ABSTRACT

Recently there have been claims on model-independent evidence of dynamical dark energy. Herein we consider a fairly general class of cosmological models with a time-evolving cosmological term of the form  $\Lambda(H) = C_0 + C_H H^2 + C_{\dot{H}} \dot{H}$ , where  $H$  is the Hubble rate. These models are well motivated from the theoretical point of view since they can be related to the general form of the effective action of quantum field theory in curved spacetime. Consistency with matter conservation can be achieved by letting the Newtonian coupling  $G$  change very slowly with the expansion. We solve these dynamical vacuum models and fit them to the wealth of expansion history and linear structure formation data. The results of our analysis indicate a significantly better agreement as compared to the concordance  $\Lambda$ CDM model, thus supporting the possibility of a dynamical cosmic vacuum.

*Subject headings:* cosmology: observations, theory (dark energy, large-scale structure of universe) — methods: numerical, statistical

### 1. INTRODUCTION

The positive evidence that our Universe is speeding up owing to some form of dark energy (DE) pervading all corners of the interstellar space seems to be nowadays beyond doubt after the first measurements of distant supernovae (Riess et al. 1998; Perlmutter et al. 1999) and the most recent analysis of the precision cosmological data by the Planck collaboration (Planck Collaboration XIII 2015). The ultimate origin of such positive acceleration is unknown but the simplest possibility would be the presence of a tiny and positive cosmological constant (CC) in Einstein’s field equations,  $\Lambda > 0$ . This framework, the so-called concordance or  $\Lambda$ CDM model, seems to describe quite well the observations (Planck Collaboration XIII 2015) but, unfortunately, there is little theoretical motivation for it. The CC is usually associated to the energy density carried by the vacuum, through the parameter  $\rho_\Lambda = \Lambda/(8\pi G)$  (in which  $G$  is the Newtonian coupling), although it is difficult to reconcile its measured value ( $\rho_\Lambda \sim 10^{-47}$  GeV<sup>4</sup>) with typical expectations in quantum field theory (QFT) and string theory, which are many orders of magnitude bigger. Such situation has triggered in the past – only to find it reinforced at present – the old CC problem and the cosmic coincidence problem (Weinberg 1989; Sahni & Starobinsky 2000; Padmanabhan 2003; Peebles & Ratra 2003). Both problems lie at the forefront of fundamental physics.

Different theoretical scenarios have been proposed since long. In this Letter we take seriously the recent observational hint that the DE could be dynamical as a means to alleviate some tensions recently observed with the  $\Lambda$ CDM (Sahni, Shafieloo & Starobinsky 2014). Specifically, we focus on the dynamical vacuum mod-

els of the form  $\Lambda(H) = C_0 + C_H H^2 + C_{\dot{H}} \dot{H}$ , in which  $H = \dot{a}/a$  and  $\dot{H} = dH/dt$  are the Hubble rate and its cosmic time derivative, with  $C_0 \neq 0$  a constant. We assume that at least one of the coefficients  $C_H$  and  $C_{\dot{H}}$  is nonvanishing. Such models possess a well-defined  $\Lambda$ CDM limit ( $C_H, C_{\dot{H}} \rightarrow 0$ ) and involve two time derivatives of the scale factor, thereby can be consistent with the general covariance of the effective action of QFT in curved spacetime. While the general structure of  $\Lambda(H)$  can be conceived as an educated phenomenological ansatz, it can actually be related to the quantum effects on the effective vacuum action due to the expanding background, in which the leading effects may generically be captured from a renormalization group equation (Solà 2008; Shapiro & Solà 2009; Solà 2013; Solà & Gómez 2015; Solà 2015). The dimensionless coefficients  $C_H$  and  $C_{\dot{H}}$  are actually related to the  $\beta$ -function of the running and are therefore naturally small. In the presence of matter conservation this is possible by letting  $G = G(H)$  be dynamical as well (Solà 2008, 2013). A generalization of  $\rho_\Lambda(H)$  with higher powers of the Hubble rate, i.e.  $H^n$  ( $n > 2$ ), has been recently used to describe inflation, see e.g. (Lima, Basilakos & Solà 2013; Solà 2015).

In the following we solve these dynamical vacuum models  $\Lambda(H)$  and test them in the light of the recent observational data, and compare their performance with the concordance  $\Lambda$ CDM model.

### 2. BACKGROUND COSMOLOGICAL SOLUTIONS

The field equations for the dynamical vacuum energy density in the Friedmann-Lemaître-Robertson-Walker (FLRW) metric in flat space are derived in the standard way and are formally similar to the ones with strictly constant  $G$  and  $\Lambda$  terms:

$$3H^2 = 8\pi G(H) (\rho_m + \rho_r + \rho_\Lambda(H)) \quad (1)$$

$$3H^2 + 2\dot{H} = -8\pi G(H) (p_\Lambda + p_r), \quad (2)$$

where  $\rho_\Lambda(H) = \Lambda(H)/(8\pi G(H))$  is the dynamical vacuum energy density,  $p_\Lambda(H) = -\rho_\Lambda(H)$ , and  $G(H)$  is the dynamical gravitational coupling. It is convenient to take into account from the beginning the effect of relativistic

sola@ecm.ub.edu  
 adriagova@ecm.ub.edu  
 jdecrupe7@alumnes.ub.edu

<sup>1</sup>High Energy Physics Group, Dept. ECM, Univ. de Barcelona, Av. Diagonal 647, E-08028 Barcelona, Catalonia, Spain

<sup>2</sup>Institut de Ciències del Cosmos (ICC), Univ. de Barcelona, Av. Diagonal 647, E-08028 Barcelona, Catalonia, Spain

TABLE 1  
BEST-FIT VALUES FOR G1-TYPE MODELS

Model	$ \frac{\Delta G}{G_0} $ (BBN,CMB), Omh <sup>2</sup>	$\Omega_m$	$\bar{\Omega}_m$ (all data)	$\nu$	$\bar{\nu}$	$\sigma_s$	$\bar{\sigma}_s$	$\chi^2/dof$	$\bar{\chi}^2/dof$	AIC	$\bar{AIC}$
$\Lambda$ CDM	-, Yes	$0.278^{+0.005}_{-0.004}$	$0.276 \pm 0.004$	-	-	0.815	0.815	828.84/1010	828.69/1010	830.84	830.69
G1	(10%,5%), Yes	$0.278 \pm 0.006$	$0.275 \pm 0.004$	$0.0015^{+0.0017}_{-0.0015}$	$0.0021^{+0.0014}_{-0.0016}$	0.797	0.784	822.82/1009	821.97/1009	826.82	825.97
$\Lambda$ CDM	-, No	$0.292 \pm 0.008$	$0.286 \pm 0.007$	-	-	0.815	0.815	583.38/604	582.74/604	585.38	584.74
G1	(10%,5%), No	$0.290 \pm 0.011$	$0.281 \pm 0.005$	$0.0008^{+0.0016}_{-0.0015}$	$0.0015 \pm 0.0014$	0.795	0.771	577.62/603	575.70/603	581.62	579.70
$\Lambda$ CDM*	-, Yes*	$0.297 \pm 0.006$	$0.293 \pm 0.006$	-	-	0.815	0.815	806.68/982	806.17/982	808.68	808.17
G1*	(10%,5%), Yes*	$0.296 \pm 0.009$	$0.287 \pm 0.004$	$0.0006 \pm 0.0015$	$0.0012^{+0.0014}_{-0.0013}$	0.803	0.770	802.66/981	799.15/981	806.66	803.15

NOTE. — The best-fitting values for the G1-type models and their statistical significance ( $\chi^2$ -test and Akaike information criterion AIC, see the text). All quantities with a bar involve a fit to the total input data, i.e. the expansion history (Omh<sup>2</sup>+BAO+SN Ia), CMB shift parameter, the indicated constraints on the value of  $\Delta G/G_0$  at BBN and at recombination, as well as the linear growth data. Those without bar correspond to a fit in which we use all data but exclude the growth data points from the fitting procedure. “Yes” or “No” indicates if Omh<sup>2</sup> enters or not the fit. The starred scenarios correspond to removing the high redshift point  $z = 2.34$  from Omh<sup>2</sup> (see text). The quoted number of degrees of freedom ( $dof$ ) is equal to the number of data points minus the number of independent fitting parameters. The fitting parameter  $\nu$  includes all data.

TABLE 2  
BEST-FIT VALUES FOR G2-TYPE MODELS

Model	$ \frac{\Delta G}{G_0} $ (CMB), Omh <sup>2</sup>	$\Omega_m$	$\bar{\Omega}_m$ (all data)	$\nu_{\text{eff}}$	$\bar{\nu}_{\text{eff}}$	$\sigma_s$	$\bar{\sigma}_s$	$\chi^2/dof$	$\bar{\chi}^2/dof$	AIC	$\bar{AIC}$
$\Lambda$ CDM	-, Yes	$0.278^{+0.005}_{-0.004}$	$0.276 \pm 0.004$	-	-	0.815	0.815	828.84/1009	828.69/1009	830.84	830.69
G2	5%, Yes	$0.278 \pm 0.006$	$0.277 \pm 0.004$	$0.0038^{+0.0025}_{-0.0023}$	$0.0043^{+0.0018}_{-0.0020}$	0.774	0.773	817.17/1008	817.26/1008	821.17	821.26
$\Lambda$ CDM	-, No	$0.292 \pm 0.008$	$0.286 \pm 0.007$	-	-	0.815	0.815	583.38/603	582.74/603	585.38	584.74
G2	5%, No	$0.287 \pm 0.011$	$0.283 \pm 0.005$	$0.0025^{+0.0026}_{-0.0025}$	$0.0030^{+0.0021}_{-0.0018}$	0.763	0.767	572.68/602	572.99/602	576.68	576.99
$\Lambda$ CDM*	-, Yes*	$0.297 \pm 0.006$	$0.293 \pm 0.006$	-	-	0.815	0.815	806.68/981	806.17/981	808.68	808.17
G2*	5%, Yes*	$0.295 \pm 0.009$	$0.289 \pm 0.005$	$0.0015^{+0.0026}_{-0.0025}$	$0.0028^{+0.0018}_{-0.0021}$	0.789	0.765	798.85/980	797.05/980	802.85	801.05

NOTE. — As in Table 1, but for G2 models with  $\xi' = 1$  so as to maximally preserve the BBN bound (see text). The effective G2-model fitting parameter in this case is  $\nu_{\text{eff}} = \nu/4$ . The constraint on  $|\Delta G/G_0|$  from CMB anisotropies at recombination is explicitly indicated.

matter, i.e.  $p_r = (1/3)\rho_r$ , together with dust ( $p_m = 0$ ). We consider the following two realizations of the dynamical vacuum model:

$$G1: \quad \Lambda(H) = 3(c_0 + \nu H^2) \quad (3)$$

$$G2: \quad \Lambda(H, \dot{H}) = 3(c_0 + \nu H^2 + \frac{2}{3}\alpha \dot{H}), \quad (4)$$

where we have redefined  $C_0 = 3c_0$ ,  $C_H = 3\nu$  and  $C_{\dot{H}} = 2\alpha$  for convenience. Model G1 is of course a particular case of Model G2, but it will be useful to distinguish between them. We can combine (1) and (2) to obtain the equation of local covariant conservation of the energy, i.e.  $\nabla^\mu(GT_{\mu 0}) = 0$ . Explicitly, since we assume matter conservation (meaning  $\dot{\rho}_m + 3H\rho_m = 0$  and  $\dot{\rho}_r + 4H\rho_r = 0$ ), it leads to a dynamical interplay between the vacuum and the Newtonian coupling:

$$\dot{G}(\rho_m + \rho_r + \rho_\Lambda) + G\dot{\rho}_\Lambda = 0. \quad (5)$$

Trading the cosmic time for the scale factor  $a$ , the previous equations amount to determine  $G$  as a function of  $a$ . Using the matter conservation equations, we arrive at

$$G(a) = -G_0 \left[ \frac{a (E^2(a))'}{3\Omega_m a^{-3} + 4\Omega_r a^{-4}} \right], \quad (6)$$

where  $G_0 \equiv G(a = 1)$  is the present value of  $G$ , and  $E(a) = H(a)/H_0$  is the normalized Hubble rate to its present value. The prime stands for  $d/da$ , and  $\Omega_i = \rho_{i0}/\rho_{c0}$  (with  $\rho_{c0} = 3H_0^2/8\pi G_0$ ) are the currently normalized energy densities with respect to the critical density. Inserting (4) and the above result for  $G(a)$  in

Eq. (1) and integrating, we obtain:

$$E^2(a) = 1 + \frac{\Omega_m}{\xi} \left[ -1 + a^{-4\xi'} \left( a + \frac{\xi \Omega_r}{\xi' \Omega_m} \right)^{\frac{\xi'}{1-\alpha}} \right], \quad (7)$$

where we have introduced

$$\xi = \frac{1-\nu}{1-\alpha} \equiv 1 - \nu_{\text{eff}}, \quad \xi' = \frac{1-\nu}{1-\frac{4}{3}\alpha} \equiv 1 - \nu'_{\text{eff}}. \quad (8)$$

For small  $|\nu, \alpha| \ll 1$  (the expected situation), we can use the approximations  $\nu_{\text{eff}} \simeq \nu - \alpha$  and  $\nu'_{\text{eff}} \simeq \nu - (4/3)\alpha$ . Note that, in order to simplify the presentation, we have removed from Eq. (7) terms proportional to  $\Omega_r \ll \Omega_m$  that are not relevant here. We can check e.g. that in the radiation-dominated epoch the leading term in the expression (7) is  $\sim \Omega_r a^{-4\xi'}$ , whilst in the matter-dominated epoch is  $\sim \Omega_m a^{-3\xi}$ . Furthermore, we find that the (full) expression for  $E^2(a)$  reduces to the  $\Lambda$ CDM form,  $1 + \Omega_m(a^{-3} - 1) + \Omega_r(a^{-4} - 1)$ , in the limit  $\nu, \alpha \rightarrow 0$  (i.e.  $\xi, \xi' \rightarrow 1$ ). Notice also the constraint among the parameters,  $c_0 = H_0^2 [\Omega_\Lambda - \nu + \alpha(\Omega_m + \frac{4}{3}\Omega_r)]$ , which follows from matching the vacuum energy density  $\rho_\Lambda(H)$  to its present value  $\rho_\Lambda^0$  for  $H = H_0$  and using  $\Omega_m + \Omega_r + \Omega_\Lambda = 1$ . The explicit scale factor dependence of the Newtonian coupling ensues upon inserting (7) in (6) and computing the derivative. We refrain once more from writing out the full expression here, but one can check that in the limit  $a \rightarrow 0$  (relevant for the Big Bang Nucleosynthesis epoch) it behaves as

$$G(a) = G_0 a^{4(1-\xi')} \simeq G_0 (1 + 4\nu'_{\text{eff}} \ln a). \quad (9)$$

Thus, the gravitational coupling evolves logarithmically with the scale factor and hence changes very slowly. This

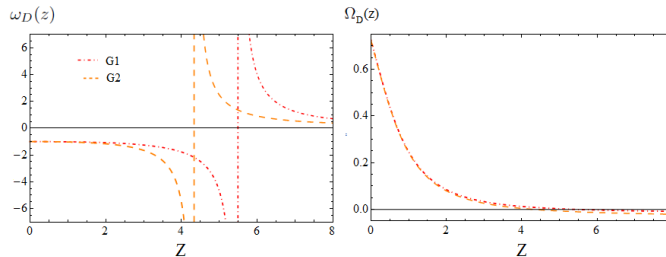


FIG. 1.— Left: Evolution of the effective EoS  $\omega_D(z)$ , Eq. (11), for the models under consideration: Right: The corresponding evolution of the effective DE density  $\Omega_D(z)$  normalized to the critical density (see text).

logarithmic law was motivated previously in (Solà 2008, 2013) within the context of the renormalization group of QFT in curved spacetime. For  $\nu = \alpha = 0$  we obtain  $G = G_0$  identically, i.e. the current value of the gravitational coupling. However the situation  $G = G_0$  is also attained in the limit  $a \rightarrow 0$  for  $\nu = (4/3)\alpha$  (i.e.  $\xi' = 1$ ); and indeed we shall adopt this setting hereafter in order to maximally preserve the BBN constraint for the G2 model. The effective fitting parameter will be  $\nu_{\text{eff}} = \nu/4$ . Obviously this setting is impossible for G1, so in this case we will adopt the average BBN restriction  $|\Delta G/G| < 10\%$  in the literature (Chiba 2011; Uzan 2011). At the same time we require  $|\Delta G/G| < 5\%$  at recombination ( $z \simeq 1100$ ) for both G1 and G2 from the CMB anisotropy spectrum (Chiba 2011).

The expression for the dynamical vacuum energy density can be obtained from Friedmann's equation (1), in combination with the explicit form of  $G(a)$ . We quote here only the simplified expression valid for the matter-dominated epoch:

$$\rho_\Lambda(a) = \rho_{c0} a^{-3} \left[ a^{3\xi} + \frac{\Omega_m}{\xi} (1 - \xi - a^{3\xi}) \right]. \quad (10)$$

For  $\xi \rightarrow 1$  we have  $\rho_\Lambda \rightarrow \rho_{c0}(1 - \Omega_m) = \rho_{c0}\Omega_\Lambda$  and we retrieve the  $\Lambda$ CDM case with strictly constant  $\rho_\Lambda$ . The form (10) is sufficient to obtain an effective DE density  $\rho_D(z)$  and effective equation of state (EoS) for the DE at fixed  $G = G_0$ , as conventionally used in different places of the literature – see e.g. (Solà & Stefancic 2006, 2005; Shafieloo et al. 2006; Basilakos & Solà 2014). We find:

$$\omega_D(a) = -\frac{1}{1 + \frac{\rho_m(a)}{\rho_\Lambda(a)} \frac{G(a) - G_0}{G(a)}}. \quad (11)$$

In Fig. 1 (left) we plot  $\omega_D$  as a function of the cosmic redshift  $z = -1 + 1/a$  for models G1 and G2. Near our time,  $\omega_D$  stays very close to  $-1$  (compatible with the  $\Lambda$ CDM), but at high  $z$  it departs. In the same Fig. 1 (right) we plot  $\Omega_D(z) = \rho_D(z)/\rho_c(z)$ , i.e. the normalized DE density with respect to the critical density at constant  $G_0$ . The asymptotes of  $\omega_D$  for each model at  $z > 4$  are due to the vanishing of  $\Omega_D(z)$  at the corresponding point (as clearly seen in the figure)– confer the aforementioned references for similar features.

### 3. FITTING THE MODELS TO THE OBSERVATIONAL DATA

Let us now test these models versus observation. First of all, we use the available measurements of the Hubble function as collected in (Ding et al. 2015). These are essentially the data points of (Farooq & Ratra 2013)

in the redshift range  $0 \leq z \leq 1.75$  and the BAO measurement at the largest redshift  $H(z = 2.34)$  taken after (Delubac 2015) on the basis of BAO's in the Ly $\alpha$  forest of BOSS DR11 quasars. We define the following  $\chi^2$  function, to be minimized:

$$\chi_{\text{Omh}^2}^2 = \sum_{i=1}^{N-1} \sum_{j=i+1}^N \left[ \frac{\text{Omh}_{th}^2(H_i, H_j) - \text{Omh}_{obs}^2(H_i, H_j)}{\sigma_{\text{Omh}^2, ij}} \right]^2, \quad (12)$$

where  $N$  is the number of points  $H(z)$  contained in the data set,  $H_i \equiv H(z_i)$ , and the two-point diagnostic  $\text{Omh}^2(z_2, z_1) \equiv [h^2(z_2) - h^2(z_1)] / [(1 + z_2)^3 - (1 + z_1)^3]$  was defined in (Sahni, Shafieloo & Starobinsky 2014), with  $h(z) = hE(z)$ , and  $\sigma_{\text{Omh}^2, ij}$  is the uncertainty associated to the observed value  $\text{Omh}_{obs}^2(H_i, H_j)$  for a given pair of points  $ij$ , viz.

$$\sigma_{\text{Omh}^2, ij}^2 = \frac{4 \left[ h^2(z_i) \sigma_{h(z_i)}^2 + h^2(z_j) \sigma_{h(z_j)}^2 \right]}{[(1 + z_i)^3 - (1 + z_j)^3]^2}. \quad (13)$$

For the  $\Lambda$ CDM the two-point diagnostic boils down to  $\text{Omh}^2(z_2, z_1) = \Omega_m h^2$ , which is constant for any pair  $z_1, z_2$ . Using this testing tool and the known observational information on  $H(z)$  at the three redshift values  $z = 0, 0.57, 2.34$  the aforementioned authors observed that the average result is:  $\text{Omh}^2 = 0.122 \pm 0.010$ , with very little variation from any pair of points taken. The obtained result is significantly smaller than the corresponding Planck value of the two-point diagnostic, which is constant and given by  $\text{Omh}^2 = \Omega_m h^2 = 0.1415 \pm 0.0019$  (Planck Collaboration XIII 2015).

A departure of  $\text{Omh}^2$  from the Planck result should, according to (Sahni, Shafieloo & Starobinsky 2014), signal that the DE cannot be described by a rigid cosmological constant. For the  $\Lambda$ CDM we obtain  $\text{Omh}^2 = 0.1250 \pm 0.0039$ , and  $\text{Omh}^2 = 0.1402 \pm 0.0059$ , by taking all data points, and excluding the high redshift one, respectively. Since there is a priori no reason to exclude the high-redshift point (Delubac 2015), whose uncertainty is one of the lowest in the full data sample, relaxing the tension with data may require the dynamical nature of the DE. The vacuum models G1 and G2 considered here, Eqs. (3,4), aim at cooperating in this task.

For these models the theoretical value  $\text{Omh}_{th}^2$  of the two-point diagnostic entering (12) can be computed, in the matter-dominated epoch (relevant for such observable), as follows:

$$\text{Omh}_G^2(z_i, z_j) = \frac{\Omega_m h^2}{\xi} \frac{(1 + z_i)^{3\xi} - (1 + z_j)^{3\xi}}{(1 + z_i)^3 - (1 + z_j)^3}. \quad (14)$$

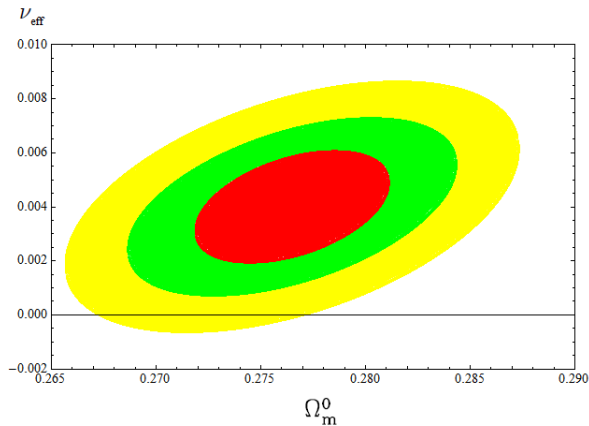


FIG. 2.— Likelihood contours in the  $(\Omega_m, \nu_{\text{eff}})$  plane (for the values  $-2 \ln \mathcal{L}/\mathcal{L}_{\text{max}} = 2.30, 6.16, 11.81$ , corresponding to  $1\sigma, 2\sigma$  and  $3\sigma$  confidence levels for the G2 model using the full data analysis indicated in Table 2. The  $\nu_{\text{eff}} = 0$  region ( $\Lambda\text{CDM}$ ) is disfavored at  $\sim 3\sigma$ .

It is evident that for  $\xi = 1$  we recover the  $\Lambda\text{CDM}$  result, which remains anchored at  $Om h^2(z_i, z_j) = \Omega_m h^2 (\forall z_i, \forall z_j)$ . However, when we allow some small vacuum dynamics (meaning  $\nu$  and/or  $\alpha$  different from zero) we obtain a small departure of  $\xi$  from 1 and therefore the DE diagnostic  $Om h^2$  deviates from  $\Omega_m h^2$ . In this case  $Om h^2$  evolves with cosmic time (or redshift).

To the above Hubble parameter data we add the recent supernovae type Ia data (SNIa), the Cosmic Microwave Background (CMB) shift parameter, the Baryonic Acoustic Oscillations (BAO's), the growth rate for structure formation (see next section) and the BBN and CMB anisotropy bounds. Contour lines for  $\nu_{\text{eff}} = 1 - \xi$  are shown in Fig. 2 for model G2 at fixed  $\xi' = 1$ . The  $\chi^2$  functions associated to SNIa distance modulus  $\mu(z)$ , the BAO  $A$ -parameter and the CMB shift parameter can be found in (Gómez-Valent, Solà & Basilakos 2015). Therein, one can also find the corresponding references of the data sets that we have used in the present analysis.

#### 4. LINEAR STRUCTURE FORMATION

Finally, we take into consideration the data on the linear structure formation. For the G1 and G2 models the calculation of  $\delta_m = \delta\rho_m/\rho_m$  is significantly more complicated than in the  $\Lambda\text{CDM}$  case and follows from applying linear perturbation theory to Einstein's field equations and Bianchi identity (5) (Grande et al. 2010). The final result reads<sup>3</sup>:

$$\delta_m''' + \frac{\delta_m''}{2a}(16 - 9\Omega_m) + \frac{3\delta_m'}{2a^2}(8 - 11\Omega_m + 3\Omega_m^2 - a\Omega_m') = 0, \quad (15)$$

with  $\Omega_m(a) = 8\pi G(a)\rho_m(a)/3H^2(a)$ . Notice that the  $(\nu, \alpha)$  model-dependence is encoded in  $H(a)$  – cf. Eqs. (7,8). To solve the above equation (numerically) we have to fix the initial conditions for  $\delta_m, \delta_m'$  and  $\delta_m''$ . We take due account of the fact that for these models at small

<sup>3</sup> The third-order feature of this equation is characteristic of the coupled systems of matter and DE perturbations for cosmologies with matter conservation, after eliminating the perturbations in the DE in favor of a single higher order equation for the matter part – cf. (Gómez-Valent, Karimkhani & Solà 2015) for details. For  $\Lambda = \text{const.}$  Eq. (15) boils down to the (derivative of the) second order one of the  $\Lambda\text{CDM}$ .

$a$  (when non-relativistic matter dominates over the vacuum) we have  $\delta_m(a) = a^s$ , where  $s = 3\xi - 2 = 1 - 3\nu_{\text{eff}}$ . If  $\xi = 1$  ( $\nu_{\text{eff}} = 0$ ), then  $\delta_m(a) \sim a$  and we recover the  $\Lambda\text{CDM}$  behavior. Thus, the initial conditions set at a high redshift  $z_i = (1 - a_i)/a_i$ , say  $z_i = 100$  (or at any higher value), are the following. For the growth factor we have  $\delta_m(a_i) = a_i^s$ , and for its derivatives:  $\delta_m'(a_i) = s a_i^{s-1}$ ,  $\delta_m''(a_i) = s(s-1)a_i^{s-2}$ .

In practice we investigate the agreement with the structure formation data by comparing the theoretical linear growth prediction  $f(z) = -(1+z)d \ln \delta_m/dz$  and the growth rate index  $\gamma(z)$  with the available growth data – following (Gómez-Valent, Solà & Basilakos 2015) and references therein. Recall that  $\gamma$  is defined through  $f(z) \simeq \Omega_m(z)^{\gamma(z)}$ , and one typically expects  $\gamma(0) = 0.56 \pm 0.05$  for  $\Lambda\text{CDM}$ -like models (Pouri, Basilakos & Plionis 2014). A most convenient related quantity is the weighted growth rate  $f(z)\sigma_8(z)$ , cf. (Song & Percival 2009), where  $\sigma_8(z)$  is the rms mass fluctuation amplitude on scales of  $R_8 = 8 h^{-1}$  Mpc at redshift  $z$ . The latter is computed from

$$\sigma_8(z) = \sigma_{8,\Lambda} \frac{\delta_m(z)}{\delta_m^\Lambda(0)} \left[ \frac{\int_0^\infty k^{n_s+2} T^2(\Omega_m, k) W^2(kR_8) dk}{\int_0^\infty k^{n_s+2} T^2(\Omega_{m,\Lambda}, k) W^2(kR_8) dk} \right]^{1/2} \quad (16)$$

$W$  being a top-hat smoothing function (see e.g. (Gómez-Valent, Solà & Basilakos 2015) for details) and  $T(\Omega_m, k)$  the transfer function, which we take from (Bardeen et al. 1986). The values of  $\sigma_8 \equiv \sigma_8(0)$  for the various models are collected in Table 1, and in Fig. 3 we plot  $f(z)\sigma_8(z)$  and  $\gamma(z)$  for them.

The joint likelihood analysis is performed on the set of  $Om h^2 + \text{BAO} + \text{SNIa} + \text{CMB}$ , BBN and linear growth data, involving one ( $\Omega_m$ ) or two ( $\Omega_m, \nu_{\text{eff}}$ ) independently adjusted parameters depending on the model. For the  $\Lambda\text{CDM}$  we have one parameter ( $n_p = 1$ ) and for G1 and G2 we have  $n_p = 2$ . Recall that for G2 we have fixed  $\xi' = 1$ .

#### 5. DISCUSSION

The main results of this work are synthesized in Tables 1-2 and Figures 1-3. In particular, from Fig. 2 we see that the model parameter  $\nu_{\text{eff}}$  for G2 is clearly projected onto the positive region, which encompasses most of the  $3\sigma$  range. Remarkably, the  $\chi^2$ -value of the overall fit is smaller than that of  $\Lambda\text{CDM}$  for both G1 and G2 (cf. Tables 1-2). To better assess the distinctive quality of the fits we apply the well known Akaike Information Criterion (AIC) (Akaike 1974), which requires the condition  $N_{\text{tot}}/n_p > 40$  (amply satisfied in our case). It is defined, for Gaussian errors, as follows:  $\text{AIC} = -2 \ln \mathcal{L}_{\text{max}} + 2n_p = \chi_{\text{min}}^2 + 2n_p$ , where  $\mathcal{L}_{\text{max}}$  (resp.  $\chi_{\text{min}}^2$ ) is the maximum (resp. minimum) of the likelihood (resp.  $\chi^2$ ) function. To test the effectiveness of models  $M_i$  and  $M_j$ , one considers the pairwise difference  $(\Delta\text{AIC})_{ij} = (\text{AIC})_i - (\text{AIC})_j$ . The larger the value of  $\Delta_{ij} \equiv |\Delta(\text{AIC})_{ij}|$ , the higher the evidence against the model with larger value of AIC, with  $\Delta_{ij} \geq 2$  indicating a positive such evidence and  $\Delta_{ij} \geq 6$  denoting significant such evidence.

From Tables 1-2 we see that when we compare the fit quality of models  $i = \text{G1, G2}$  with that of  $j = \Lambda\text{CDM}$ ,

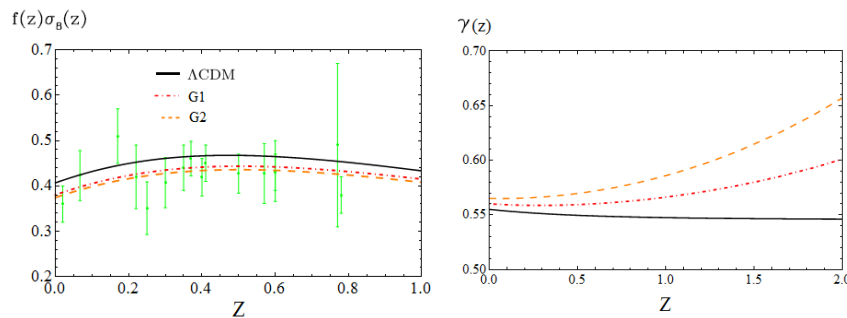


FIG. 3.— Left: Comparison of the observed data with error bars (in green) and the theoretical evolution of the weighted growth rate of clustering  $f(z)\sigma_8(z)$  for each dynamical vacuum model and the  $\Lambda$ CDM. Right: The corresponding evolution of the linear growth index  $\gamma(z)$ .

in a situation when we take all the data for the fit optimization, we find  $\overline{\Delta_{ij}} \equiv \overline{\Delta \text{AIC}} \gtrsim 9.43$  for G2 and 4.72 for G1, suggesting significant evidence in favor of these models (especially G2) against the  $\Lambda$ CDM – the evidence ratio (Akaike 1974) being  $ER = e^{\overline{\Delta_{ij}}/2} \gtrsim 111.6$  for G2 and 10.6 for G1. Worth noticing is also the result of the fit when we exclude the growth data from the fitting procedure but still add their contribution to the total  $\chi^2$ . This fit is of course less optimized, but allows us to risk a prediction for the linear growth and hence to test the level of agreement with these data points (cf. Fig. 3). It turns out that the corresponding AIC pairwise difference with the  $\Lambda$ CDM are similar as before (cf. Tables 1-2). Therefore, the  $\Lambda$ CDM appears significantly disfavored versus the dynamical vacuum models, especially in front of G2, according to the Akaike Information Criterion. Let us mention that if we remove all of the  $H(z)$  data points from our analysis the fit quality weakens, but it still gives a better fit than the  $\Lambda$ CDM (cf. the third and fourth row of Tables 1 and 2). If, however, we keep these data points but remove *only* the high redshift point  $z = 2.34$  (Delubac 2015), the outcome is not dramatically different from the previous situation (confer the starred scenarios in Tables 1 and 2), as in both cases the significance of  $\nu_{\text{eff}} \neq 0$  is still close to  $\sim 2\sigma$  with  $\Delta_{ij} > 7$  for G2 (hence still strongly favored, with

$ER > 33$ ). In this sense the high  $z$  point may not be so crucial for claiming hints in favor of dynamical vacuum, as the hints themselves seem to emerge more as an overall effect of the data. While we are awaiting for new measurements of the Hubble parameter at high redshift to better assess their real impact, we have checked that if we add to our analysis the points  $z = 2.30$  (Busca et al. 2013) and  $z = 2.36$  (Font-Ribera et al. 2014), not included in either (Sahni, Shafieloo & Starobinsky 2014) or (Ding et al. 2015), our conclusions remain unchanged. Ditto if using the three high  $z$  points only.

To summarize, our study singles out a general class of vacuum models, whose dynamical behavior challenges the overall fit quality of the rigid  $\Lambda$ -term inherent to the concordance  $\Lambda$ CDM model. From the data on expansion, structure formation, BBN and CMB observables we conclude that the  $\Lambda$ CDM model is currently disfavored at  $\sim 3\sigma$  level as compared to the best dynamical ones.

## 6. ACKNOWLEDGEMENTS

We thank the anonymous referee for his/her thorough report on our work and for very useful suggestions to improve our analysis. JS has been supported in part by MICINN, CPAN and Generalitat de Catalunya; AGV acknowledges support by APIF grant of the U. Barcelona.

## REFERENCES

- Ade, P.A.R., et al. [Planck Collaboration], *Planck 2015 results. XIII. Cosmological parameters*, arXiv:1502.01589.
- Akaike, H. IEEE Transactions of Automatic Control, 19 (1974) 716; N. Sugiura, Communications in Statistics A, Theory and Methods, 7 (1978) 13; K.P. Burnham & D.R. Anderson, *Model selection and multimodel inference* (Springer, New York, 2002).
- Bardeen, J. M., Bond, J. R., Kaiser, N., & Szalay, A. S., ApJ **304** (1986) 15.
- Basilakos, S., & Solà, J., Mon. Not. Roy. Astron. Soc. **437** (2014) 3331
- Busca, N.G. et al., A&A **552** (2013) A96.
- Chiba, T., Prog. Theor. Phys. **126** (2011) 993; Nagata, R., Chiba, T., & Sugiyama, N., Phys. Rev. D **69** (2004) 083512.
- Delubac, T., et al., A&A **574** (2015) A59.
- Ding, X., et al., ApJ **803** (2015) L22.
- Farooq, O., & Ratra, B., ApJ **766** (2013) L7.
- Font-Ribera, A. et al., JCAP **05** (2014) 027.
- Gómez-Valent, A., Solà, J., & Basilakos, S., JCAP **01** (2015) 004; A. Gómez-Valent & J. Solà, MNRAS **448** (2015) 2810.
- Gómez-Valent, A., Karimkhani, E., & Solà, J., work in preparation.
- Grande, J., et. al, Class. Quant. Grav. **27** (2010) 105004; JCAP **08** (2011) 007.
- Lima, J. A. S., Basilakos, S., & Solà, J., MNRAS **431** (2013) 923; Gen. Rel. Grav. **47** (2015) 40.
- Padmanabhan, T., Phys. Rept. **380** (2003) 235.
- Peebles P.J.E., & Ratra, B., Rev. Mod. Phys. **75** (2003) 559.
- Perlmutter, S., et al. ApJ **517** (1999) 565.
- Pouri, A., Basilakos, S., & Plionis, M., JCAP **08** (2014) 042.
- Riess, A. G., et al., Astron. J. **116** (1998) 1009.
- Sahni, V., Shafieloo, A., & Starobinsky, A. A., ApJ **793** (2014) L40.
- Sahni, V., & Starobinsky, A. A., Int. J. of Mod. Phys. A **9** (2000) 373.
- Shafieloo, A., Alam, U., Sahni, V., Starobinsky, A. A., Mon. Not. Roy. Astron. Soc. **366** (2006) 1081.
- Shapiro, I. L., & Solà, J., Phys.Lett. **B682** (2009) 105; JHEP **02** (2002) 006.
- Solà, J., J. of Phys. A **41** (2008) 164066.
- Solà, J., J. Phys. Conf. Ser. **453** (2013) 012015.
- Solà, J., & Gómez-Valent, A., Int.J.Mod.Phys. **D24** (2015) 1541003.
- Solà, J., arXiv:1505.05863 (to appear in Int. J. of Mod. Phys. D).
- Solà, J., & Stefancic, H., Mod. Phys. Lett. **A21** (2006) 479; Phys.Lett. **B624** (2005) 147.
- Song, Y.-S., & Percival, W.J., JCAP **10** (2009) 004.
- Uzan, J.-P., Living Rev.Rel. **14** (2011) 2.
- Weinberg, S., Rev. Mod. Phys. **61** (1989) 1.